TAO, Vol. 9, No. 3, 453-472, September 1998

Structural Controls of the Taitung Canyon in the Huatung Basin East of Taiwan

Philippe Schnürle[1], Char-Shine Liu[1], Serge E. Lallemand[2], and Donald Reed[3]

(Manuscript received 10 March 1998, in final form 3 September 1998)

ABSTRACT

The Taitung Canyon originates at the southern end of the Longitudinal Valley. It runs southward along the axis of the Taitung Trough. The canyon turns eastward into the Huatung Basin, after crossing the Luzon arc between the volcanic islands of Lanyu and Lutao. It then flows northeastward for about 170 km and merges with the Hualien Canyon near the Ryukyu Trench, thus forming the largest canyon in the Huatung Basin. High resolution bathymetric data, and several multi-channel seismic profiles are used to describe the structural fabric in the vicinity of the Taitung Canyon and the factors controlling its path within the Huatung Basin. Crossing the eastern slope of the Lanyu-Lutao volcanic ridge, the head of the Taitung Canyon is fan shaped and its entrenchment rapidly increases downslope. Throughout the canyon's upper and central portions, the channel depth ranges from 300 to 500 m with respect to the surrounding seafloor. The canyon's levees are generally asymmetric and turbidite overbank deposits are observed. Then, a basement high, trending parallel to the Gagua Ridge, forces the path of the Taitung Canyon to turn 90° toward the northwest. As the canyon reaches the Ryukyu Trench, the width of the main channel has decreased from 14 km near the Luzon arc, to less than 200 m at the outer-slope of the Ryukyu Trench. The importance of structural controls, such as basement highs and faulting, on the canyon's development are examined. Thus, the existence of a strike-slip fault system, affecting the oceanic basement in the Huatung Basin, and its role in controlling the path of the canyon are discussed.

(Key words: Submarine canyon, Seismic reflection profiles, Huatung Basin, Taiwan)

1. TECTONIC SETTING

The island of Taiwan is located at the junction of the Ryukyu and Luzon island arcs along

[1] Institute of Oceanography, National Taiwan University, Taipei, Taiwan, ROC

[2] Laboratoire de Géophysique et Tectonique, Université de Montpellier II, 34095 Montpellier Cedex 05, France

[3] Department of Geology, San Jose State University, San Jose, CA 95192, USA

the western margin of the Philippine Sea (Figure 1). East of Taiwan, the Philippine Sea plate subducts northward underneath the Eurasian plate along the Ryukyu subduction system, while south of Taiwan, the Eurasian plate in the South China Sea subducts eastward underneath the Philippine Sea plate along the Manila subduction zone (Karig, 1973; Bowin *et al.*, 1978; Angelier, 1986). Between these two systems, the orogen of Taiwan results from the collision of the Luzon volcanic arc with the passive Chinese continental margin since Pliocene time (Biq, 1972; Ho, 1986; Teng, 1990).

The obliquity of the plate convergence, (307° N versus 350-10° trend of the collision zone, at a rate of about 7 cm/yr; Seno *et al.*, 1993), results in a southward propagation of the collision (Suppe, 1987). A mature stage is observed along the Coastal Range, the onland portion of the Luzon arc in eastern Taiwan (Ho, 1986), while south of Taiwan, the closure of the Luzon forearc basin and the thrusting of the Huatung ridge over the Luzon Arc are regarded as initial stages of the collision (Lundberg *et al.*, 1992; 1997; Huang *et al.*, 1992; Reed *et al.*, 1992; Malavieille *et al.*, 1997). According to GPS measurements (Yu *et al.*, 1997), while south of 24°N, the plate convergence is distributed across southern and central Taiwan, the mountain building process has apparently ended in northern Taiwan (Yu and Chen, 1994), and may be evolving into an extensional regime associated with the Ryukyu back-arc system (Teng, 1995).

The Huatung Basin is located at the northwestern corner of the Philippine Sea Plate (Figure 1). The basin is bounded to the west by the Luzon arc which is formed by island arc volcanism related to the Manila subduction zone. To the east, the Huatung Basin is separated from the West Philippine Basin by a north-south trending ridge, the Gagua Ridge, along the 123°E meridian. The Gagua Ridge is about 350 km in length and 20 to 30 km wide with a maximum relief of nearly 2500 m above the sea floor. It extends from about 20°N northward into the Ryukyu Trench where it is subducting beneath the forearc region (Schnürle *et al.*, 1998; Dominguez *et al.*, submitted). The West Philippine Basin was opened in a NE-SW direction from 60 to 45 Ma, and later in a N-S direction until 35 Ma. The Huatung Basin exhibits E-W Eocene magnetic anomalies related only to the later stage of spreading (anomalies 16 to 19; Hilde and Lee, 1984). The Gagua Ridge has formed along a transform fault that offsets these two oceanic domains by 150 km (Mrozowski *et al.*, 1982; Hilde and Lee, 1984), and is likely to be an upfaulted sliver of oceanic crust (Karp *et al.*, 1997; Deschamps *et al.*, 1997).

During the Taiwan orogeny, abundant coarse sediments, eroded from the Central Range and the Coastal Range, have been funneled to the sea. Thus, large volumes of sediment derived from the Taiwan mountain belt are transported in the Huatung Basin along several submarine canyons (Figure 1). The Taitung Canyon is the most prominent one. This canyon originates at the southern end of the Longitudinal Valley near Taitung. It then runs southward along the axis of the northern Taitung Trough (e.g. Ma, 1947; Lundberg, 1988), between the Huatung Ridge (to the east) and the Luzon Arc (to the west). Samples cored at the head of the Taitung Canyon, in the Taitung Trough, contain mainly angular metamorphic detritus (Huang *et al.*, 1992). At a latitude of 22°25'N, the Taitung Canyon turns sharply eastward through a topographic low in the Luzon island arc, between the Lanyu and Lutao islands (Figure 1). From this point, the canyon extends northeastward across the Huatung Basin for 170 km, before

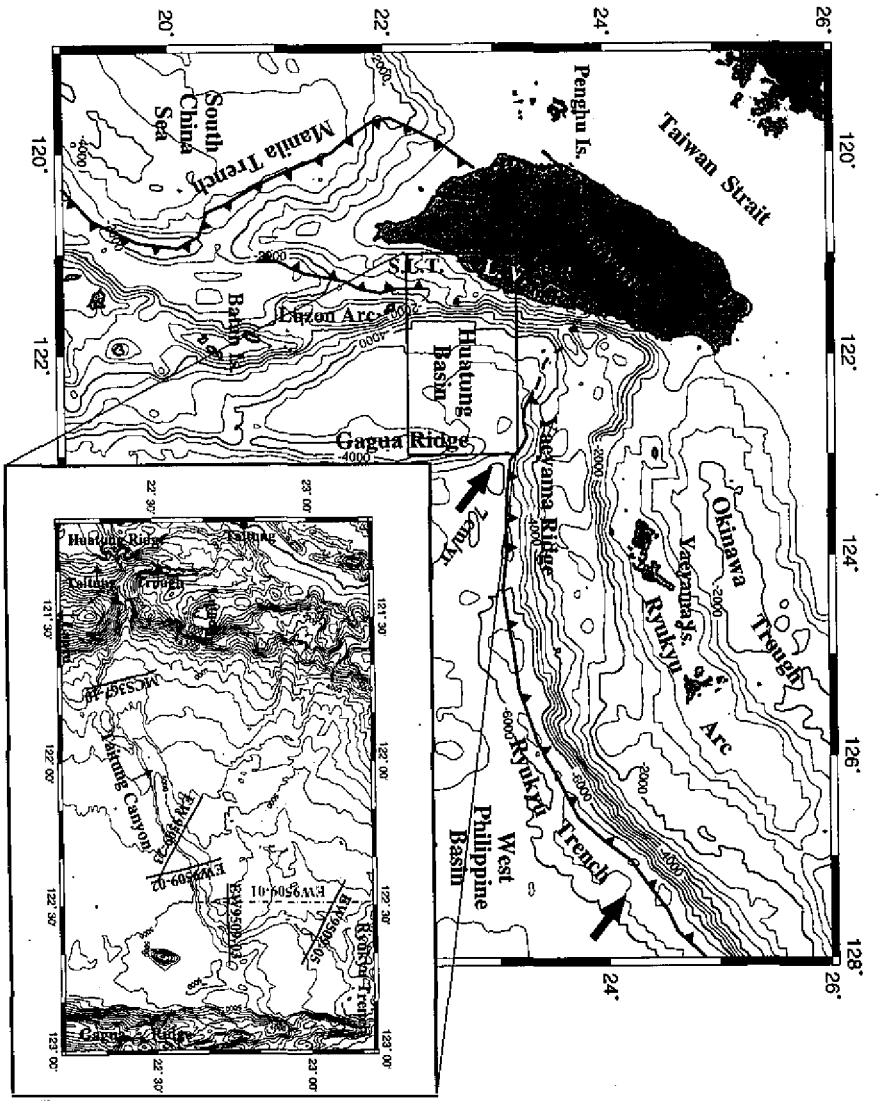

Fig. 1. Geodynamic framework of the Philippine Sea - Eurasia plate boundary in the vicinity of Taiwan. Relative plate convergence vectors are after Seno et al. (1993). Isobaths are in 500 m. Co. R. stands for Coastal Range, Ce. R. for Central Range, and L. V. for Longitudinal Valley. Inset figure shows the path of the Taitung Canyon in the Huatung Basin. Isobaths are in 200 m contours. Location of the multi-channel seismic profiles ORI367-10 (profile 1), and EW9509-23 (profile 2), EW9509-02 (profile 3), EW9509-03 (profile 4), EW9509-05 (profile 5), and EW9509-01 are given. Thick lines indicate the portion of the seismic profiles shown in Figures 2, 5 and 6.

ending near the intersection of the Gagua Ridge with the Ryukyu Trench.

The Taitung Canyon west of the Luzon Arc was originally described by Ma (1947; 1963) and its development during closure of the forearc basin was extensively described (e.g. Lundberg, 1988; Lundberg *et al.*, 1997; Malavieille *et al.*, 1997). Therefore, the aim this study is to describe and analyze the structure of the Taitung Canyon east of the Luzon arc, herein called the head of the Taitung Canyon, and its path within the Huatung Basin. This study examines the structures and sedimentary features of the Huatung Basin in the vicinity of the Taitung Canyon with special interest focused on the tectonic significance of this canyon.

2. OFFSHORE GEOPHYSICAL DATA

High resolution swath bathymetry and multichannel seismic reflection data, as well as seismicity data are analyzed in this study. Bathymetry data are based on the new digital bathymetric model (Liu *et al.*, this issue) of the study area. The multichannel seismic reflection data presented in this study were collected onboard the R/V Maurice Ewing (Cruise EW9509) during the TAICRUST survey (Liu *et al.*, 1995), and during the R/V Ocean Researcher I cruise ORI367.

During the ORI367, three Bolt airguns with volumes of 500, 300, and 120 in^3 provided the seismic energy. Seismic signals were received by a 1500 m long, 60-channel streamer and recorded by a DFS-V system on board the R/V Ocean Researcher I. For the EW9509 cruise, the seismic source was a 20-airgun array with a total volume of 8420 in^3 fired at 20 second intervals. Record lengths of 16 seconds where received by a 160-channel digital streamer with a length of 4000 m. These data sets were processed using both SIOSEIS and ProMAX seismic processing software at the Institute of Oceanography, National Taiwan University.

Along each profile, stacking velocities were interactively analyzed at every 100th common-mid-point (CMP) based on maximum semblance of a 6-CMP super-gather. Velocity picks were interpolated along the sea floor as well as the top of the oceanic basement to a regular velocity grid of evry 20th CMP (300 m horizontal) and 48 ms (71-168 m vertical) spacing. Based on the velocity field, Q compensation was applied to recover frequency-amplitude attenuation of the seismic wave field. A spiking predictive Wiener-Levinson operator was used to enhance the source signal and true amplitude recovery was performed. Frequency analysis revealed a frequency content centered around 40 Hz with -25 dB offset below 4 Hz and above 70 Hz. A minimum phase Ormsby band pass filter with corner frequencies of 3-8-70-90 Hz was applied.

Following a final stack, a migration velocity field was derived by using 80% of the stacking velocities and filtered between 1485 m/s and 3500 m/s. Fast explicit finite difference post-stack time migration (Soubaras, 1992) was performed to generate final seismic sections.

3. MORPHOLOGY AND STRUCTURAL FRAMEWORK OF THE TAITUNG CANYON EAST OF THE LUZON ARC

The Taitung Canyon extends for 170 km from its head between Lanyu and Lutao islands to the Ryukyu Trench (Figure 1). It flows in water depths ranging from 4000 to 6000 m,

however, through most of its length, the water depth is close to 5000 m. The widest portion of the canyon reaches 14 km at the foot of the Luzon arc while the width narrows to only 200 m near the Ryukyu Trench. The canyon incises the Huatung Basin and the channel depth (the vertical relief from the axis of the channel floor to the levee crest) ranges between 200 and 500 m.

Figure 2 presents the local topographic slope in the Huatung Basin. Local slopes are computed from a bathymetric grid with a 70 m grid spacing. A two-dimensional least square fit is performed over 10 x 10 pixels (700 x 700 m) and the dip along the fitted plane is extracted. Local slopes are generally lower then 0.3°. The sharp entrenchment of the canyon produces clear edges in this type of representation. The canyon's overall sinuosity, defined as the ratio of the length of the channel to the down-valley distance, is 1.26. Four sections can be identified in the path of the Taitung Canyon in the Huatung Basin (Figures 1 and 2): the head of the canyon (section 1, between 121°35'E-122°E), the upper portion (section 2, between 122°E-122°20'E), the central portion (section 3, between 122°20'E-122°40'E), the lower portion (section 4, between 122°40'E-123°E).

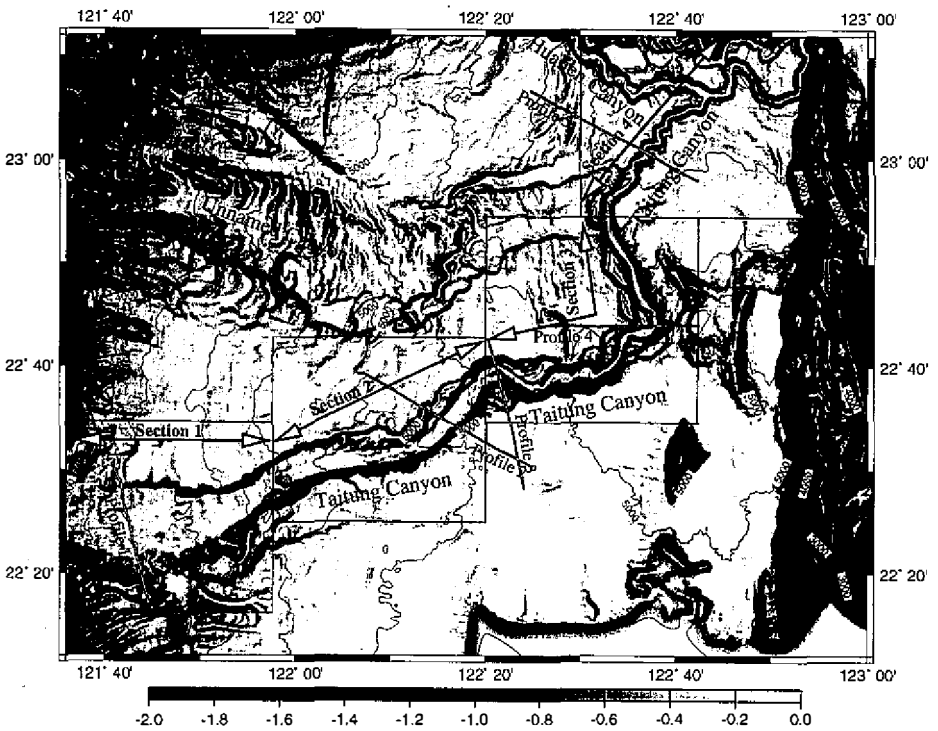

Fig. 2. View of the local bathymetric slopes, between 0 and 2 degrees, in the Huatung Basin. The Taitung submarine canyon is divided into four sections: Boxes indicate locations of the bathymetric shaded views presented in Figures 3, 5, 7 and 10. Thick white lines indicate the portions of the seismic profiles shown in Figures 2, 4 and 6.

3.1 Section 1

The canyon drops by 2000 m from the floor of the Taitung Trough, into the Huatung Basin. The head of the Taitung Canyon is fan shaped, as the flow converges from between the two volcanic islands of Lanyu and Lutao to form the entrenched canyon in the Huatung Basin. Figure 3 presents a perspective shaded view of the head of the canyon. In this section, the channel width decreases from 14 km down to 7.2 km, while the channel depth progressively increases. The floor of the canyon appears to be very rough (Figure 3) and has an average dip of 1° (from 4100 m to 4900 m in depth) while the sinuosity remains low (1.04).

Seismic profile 1 extends across the center of this section (Figure 4). A sedimentary ridge, 500 m in height on this profile, forms the southern levee of the canyon. A series of terraces (less then 100 m in height) is imaged on the northern side. By the eastern edge of this section, relief of 300 m on the northern levee and 480 m on the southern levee are observed. On seismic profile 1 (Figure 4), the channel floor is characterized by heavy disruptions: few continuous reflectors are imaged underneath the canyon floor and diffraction points are numerous, mostly near the southern levee, because the line does not cross the canyon perpendicular to its strike. Thus many out-of-plan reflection disrupt this section.

An unconformable stratum lies at 0.8 s TWT beneath the canyon floor. This unconformity extends over most of the Huatung Basin (Liu *et al.*, 1997) and is referenced as the basin-wide "unconformity Y" through-out this paper. It is marked by a dashed line on seismic profiles 1, 2, 3, 4 and 5. The unconformity Y separates the sedimentary strata into a more transparent upper layer and a coherent, continuous reflective lower layer (Liu *et al.*, 1997a). While the stratigraphy appears concordant in most of the Huatung Basin, a strong onlap of the upper layer characterizes this unconformity along the eastern flank of the submarine Luzon arc, as imaged along several east-west seismic profiles in the Huatung Basin. Depending on the age of the unconformity Y and the nature of the sediments below it, this unconformity could represent the boundary between the post- and pre-collision deposits, or, if both the upper and lower strata consist of orogenic sediments from the Taiwan mountain belt, it might imply that the Taiwan collision evolved through a two-stage processes (Liu *et al.*, 1997a).

The top of the oceanic basement lies rather continuously 1 s TWT underneath the unconformity Y. The transition from sediments to oceanic basement is characterized by high amplitude, long wavelength reflections. Few continuous reflectors can be imaged within the oceanic crust. Finally, a large offset in the oceanic basement, about 0.2 ms TWT, is observed 4 km north of the southern levee.

A second unconformity, referenced as the "Unconformity X", has been identified (Malavieille *et al.*, 1997; Liu *et al.*, 1997a) and is marked by a dashed-doted line on profiles 1, 2, 3, and 4. This unconformity is characterized by recently deposited sediments, often showing sediment waves structures, with low amplitude reflectivity on the seismic sections. Along the eastern flank of the submarine Luzon arc, these sediments lie with a clear divergent depositional pattern on top a flat strata of strong reflectivity. Within the upper layer, slide-block structures are imaged in the seismic profiles at these locations (Liu *et al.*, 1997a). It has been proposed that this unconformity acts as a basal detachment for the upper sedimentary layer in the area located between the Luzon arc and the Taitung Canyon (Malavieille *et al.*, 1997).

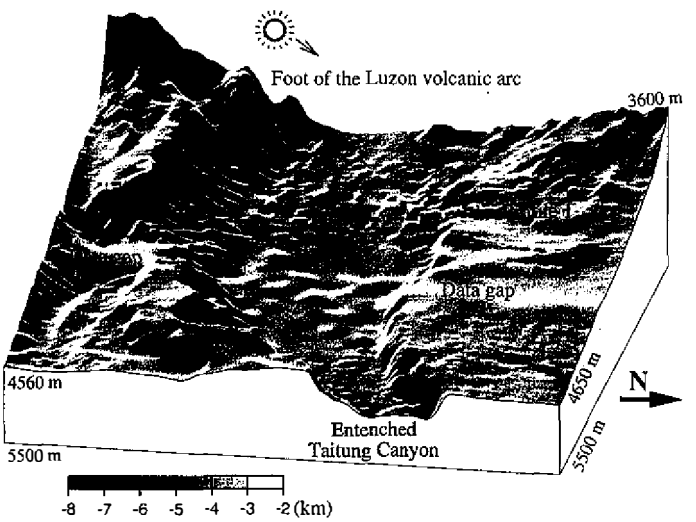

Fig. 3. Perspective shaded view of head of the Taitung Canyon (section 1) as it enters the Huatung Basin between the volcanic islands of Lanyu and Lutao (see Figure 2 for location). The view is from the east (N80°), with a 20° elevation and N250° illumination angle. Water depths at the corners are indicated. The location of seismic profile 1 (line ORI367-10) is indicated by a dashed line. A gap in the swath bathymetric coverage has occurred in the center of this box.

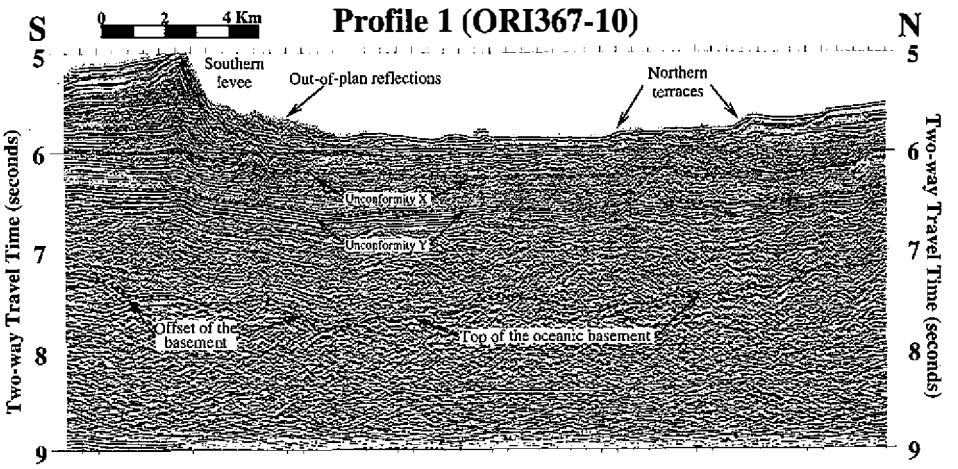

Fig. 4. Time-migrated seismic section of profile 1 (line ORI367-10). This profile runs SSE-NNW (see Figure 2 for location) across the head of the Taitung Canyon. Vertical exaggeration at sea-floor is about 2x.

On seismic profile 1, the unconformity X lies 0.35 s TWT beneath the floor of the Taitung Canyon and 0.35 s TWT above the basin wide unconformity Y. This unconformity X is best expressed beneath the northern terraces imaged on profile 1).

3.2 Section 2

Figure 5 presents a perspective shaded view of the Taitung Canyon for section 2. The channel floor has an average slope of 0.76° (from 4900 m to 5350 m in depth). The sinuosity in this section is 1.07. The channel width remains constant (9 km) in this section. The canyon retains an asymmetric levee height, with about 330 m on the northern side and 500 m on the southern side over most of this section. The northern flank of the channel is composed of a series of narrow terraces, each about 150 m in height. Due to the Coriolis forces, turbidity currents are diverted by deposition to the right side of fan-valleys in the northern hemisphere, producing a "left hook" tendency for the canyon (e.g. Menard, 1955; Shepard and Dill, 1966).

On the seismic profile 2 (Figure 6), the sediments on either side of the Taitung Canyon are flat with very low reflectivity within the upper strata. Furthermore, reflectors are abruptly truncated at the flanks of the channel. On the north-western side of the Taitung Canyon, the unconformity X is clearly imaged in this seismic section, 0.5 s TWT underneath the surrounding sea-floor. The unconformity X separates a series of continuous high amplitude reflectors from a more transparent strata. Underneath the Taitung Canyon, the seismic stratigraphy becomes unclear. The existence and location of this unconformity X becomes uncertain to the south-east of the Taitung Canyon. Then, 1.33 s TWT beneath the sea-floor in the north-west portion of seismic profile 2 and 0.67 s TWT beneath the sea-floor in the south-eastern portion, the unconformity Y is imaged at the transition between the low amplitude upper layer and the high amplitude continuous strata resting on the top of the oceanic basement. The oceanic basement is asymmetric on seismic profile 2. It lies around 7.7 s TWT south of the canyon and 7.3 s TWT on the north side. A distinctive basement depression, down to 8.3 s TWT, is imaged at the upright of the southern levee of the canyon.

Based on the seismic facies of the sequences at the flanks and floor of the canyon, the sediments within the canyon vary considerably between sections 1 and 2. Turbidite overbank deposits (overspilling) appear to be the dominant mechanism responsible for the finer grained distal deposit in the surrounding Huatung Basin. The asymmetry in the shape of the canyon's flanks might be related to the curvature in the canyon's path in this section (with a minimum radius of 16 km) with overspilling occurring preferentially along the outer (southern) side of the bend. The turn could be related to the basement high in the subsurface located south-east of the canyon.

3.3 Section 3

The central portion of the Taitung Canyon is characterized by a much larger sinuosity of 1.6 and a lower gradient of 0.6° (from 5400 m to 5780 m in depth; Figure 1 and 2). The asymmetric shape of the canyon walls also increases. In the center of this section, the canyon turns 90° from a E-NE to N-NW direction (Figure 2 and 7) which also marks the increases in sinuosity and asymmetry of canyon flanks. Within this section, the channel width decreases by

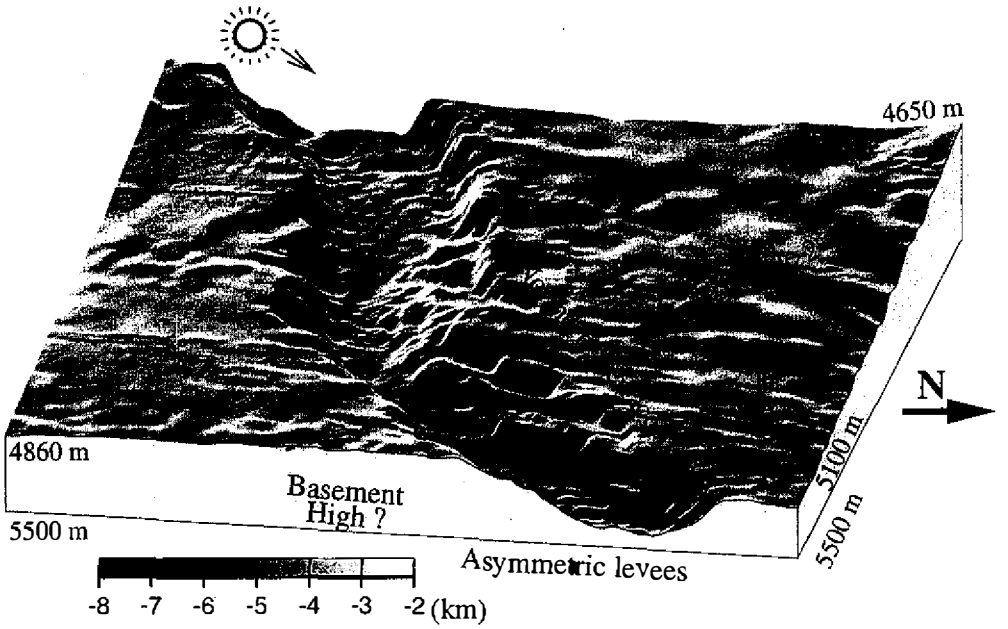

Fig. 5. Perspective shaded view of upper portion of the Taitung Canyon (section 2; see Figure 2 for location). The view is from the east (N80°), with a 20° elevation and N250° illumination angle. Water depths at the corners are indicated. The location of seismic profile 2 (line EW9509-23) is indicated by a dashed line.

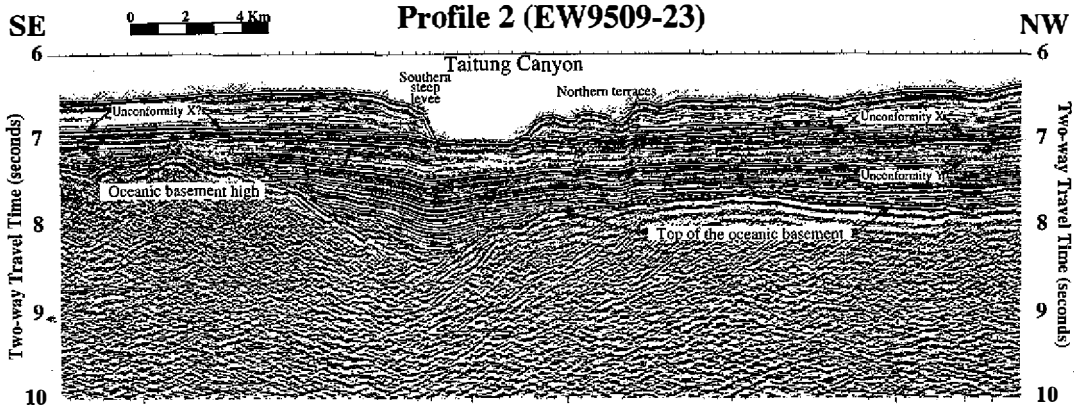

Fig. 6. Time-migrated seismic section of profile 2 (line EW9509-23). This profile runs SE-NW (see Figure 2 for location) across the upper portion of the Taitung Canyon. Vertical exaggeration at sea-floor is about 2x.

a factor of 2, from 9 km to 4.5 km.

Seismic profile 3 (Figure 8) is located at the beginning of the central portion where the path of the canyon makes a right turn (with a radius of about 5 km). The seismic imaging along this profile is similar to profile 2: 0.5 s TWT thick sequence of flat lying reflectors of low amplitude are resting on continuous high amplitude reflectors. The sequence boundary also coincides with the floor of the canyon. However, the asymmetry in the flank's shape is reversed to that of previously described sections: the northern levee is steep while terraces form along the southern levee. This suggests again that the overbanking preferentially occurs to the outer-side during turns. The existence and location of unconformity X, as on seismic profile 2, is uncertain to the south of the Taitung Canyon. Then, the basin-wide unconformity Y is imaged underneath and north of the canyon. The top of the oceanic basement lies at 7.4 s TWT in the southern part of the profile, increases in depth underneath the canyon, and rises to 7.8 s TWT at the northern edge of the profile. The largest offset in the oceanic basement (0.25 s TWT) is located south of the canyon.

Seismic profile 4 (Figure 9) runs east-west to the north of the 90° left turn (with a radius of 5 km) of the canyon, in the center of section 3. In this seismic profile, the seismic stratigraphy is generally continuous, with several normal faults particularly well expressed underneath the Taitung Canyon. Unconformities X and Y are indicated. This section is characterized by a 20 km wide trough, 1.4 to 1.6 s TWT deep, in the oceanic basement. The eastern wall of the Taitung Canyon rests against the basement flank with over-bank deposits extending over the basement high. Two basement ridge segments, located at the eastern edge of this section, rise several hundred meters above the surrounding sea-floor as shown on the bathymetry diagrams (Figure 2 and 7). These highs block the E-W flow of the Taitung Canyon, forcing its path to turn toward the NNW.

3.4 Section 4

The Taitung Canyon bends to the NE in the region adjacent to the outer-slope of the Ryukyu Trench. Several unnamed submarine channels merge into the canyon. The canyon's width decreases considerably (3.6 to 2 km) in section 4 and meandering increases (Figure 10). The sinuosity reaches 1.34 across a sea-floor of 0.4° slope (from 5700 m to 6000 m in the Ryukyu Trench). The channel depth throughout this section is about 200 m. As the Taitung Canyon approaches the Ryukyu Trench, the canyon merges with another major submarine canyon, the Hualien Canyon. The Hualien submarine canyon originates at the northern extremity of the Longitudinal Valley, near the city of Hualien. This canyon flows to the SSE, between the toe of the Yaeyama Ridge and the eastern flank of the Coastal Range. It is then joined by the Chimei submarine canyon at 122°E 23°30'N before turning to the ESE along the deformation front of the Ryukyu Trench.

Seismic profile 5 (Figure 11) clearly shows the decrease in size of the Taitung Canyon after extending 150 km across the Huatung Basin. At the south-eastern end of the profile, the top of the basement lies at 8 s TWT, consistent with a N-S oriented basement high that runs parallel to the Gagua Ridge (Figure 1). The basement depth progressively deepens to 9.7 s TWT in the center of the profile, but abruptly rises by almost 1 s TWT at the northwestern end

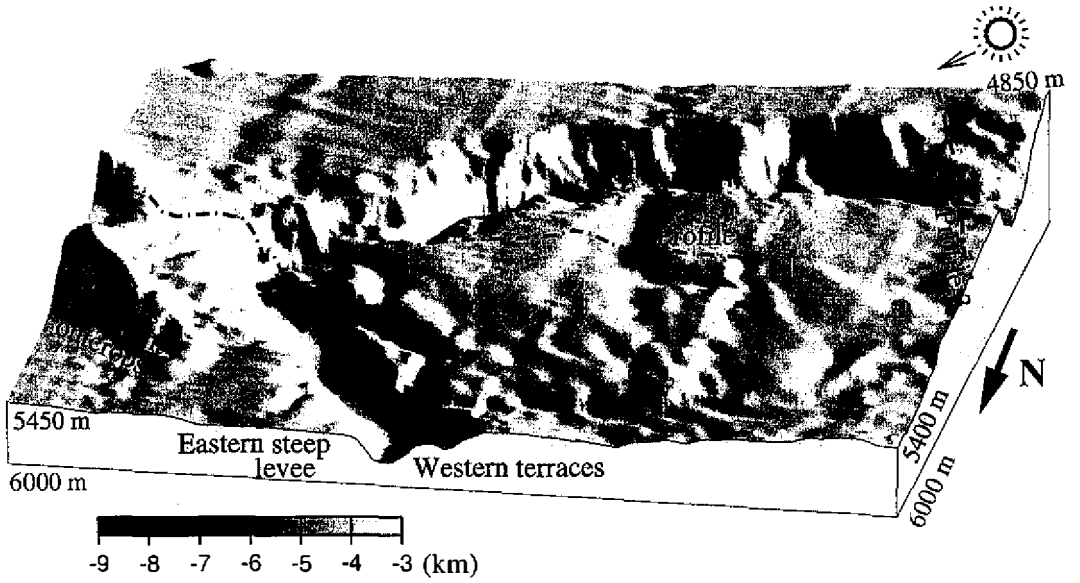

Fig. 7. Perspective shaded view of central portion of the Taitung Canyon (section 3; see Figure 2 for location). The view is from the north (N350°), with a 20° elevation and N250° illumination angle. Water depths at the corners are indicated. The locations of seismic profiles 3 (line EW9509-02) and 4 (line EW9509-03) are indicated by dashed lines.

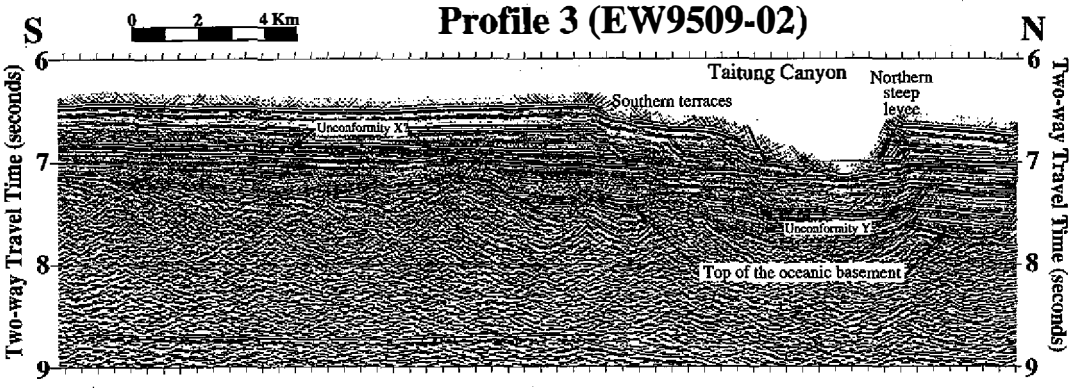

Fig. 8. Time-migrated seismic section of profile 3 (line EW9509-02). This profile runs SSE-WNW (see Figure 2 for location) across a right turn to the beginning of the central portion of the Taitung Canyon. Vertical exaggeration at sea-floor is about 2x.

of profile 5. The overlying sediments are flat-lying and undeformed. Unconformity Y lies 0.75 s TWT underneath the sea-floor. Beneath the channel's present location, evidences of older channel systems extend down to 8.5 s TWT. The Chimei and Hualien submarine canyons, (rather than the Taitung Canyon), are liable to have transported detritus to produce the thick trench fill at any sequences in this region. No age control is available for the sediment, therefore the timing of the canyon's migrations is not known.

4. DISCUSSION

With the increasing use of multibeam bathymetric (e.g. Hagen *et al.*, 1994; Hagen *et al.*, 1996; Pratson and Ryan, 1996; Pratson and Edwards, 1996; Baraza *et al.*, 1997) and swath mapping side-scan sonar systems (e.g. Damuth *et al.*, 1988; Klaus and Taylor, 1991; Liu *et al.*, 1993; Pratson and Edwards, 1996), our comprehension of submarine canyons has greatly improved. Besides commonly mentioned eustatic and erosional processes, tectonic processes exert a major influence on the origin and evolution of submarine canyons (e.g. Carlson and Karl, 1988; Greene *et al.*, 1991; Yu and Chiang, 1997). For example, structural controls on canyon development, such as basement highs, faulting, and oversteepened slopes all influence canyon morphology (Soh *et al.*, 1990). It also has been proposed that submarine canyons can form along faults, presumably because the shearing associated with the fault displacement trends to fracture rocks, so that it is less resistant to erosion (Nagel *et al.*, 1986; Greene *et al.*, 1991). The structural data presented in this study appear to be sufficient to test these hypotheses.

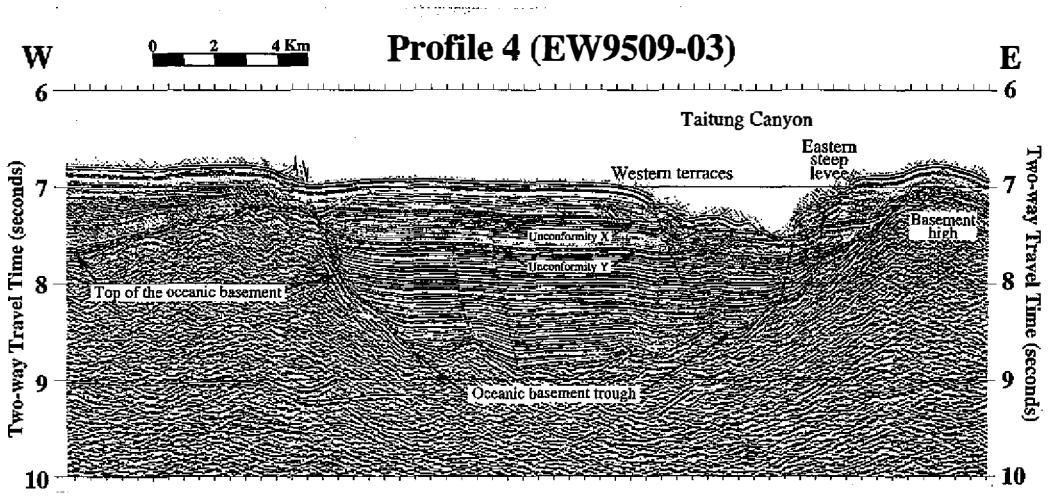

Fig. 9. Time-migrated seismic section of profile 4 (line EW9509-03). This profile runs E-W (see Figure 2 for location) a sharp left turn in the central portion of the Taitung Canyon. Vertical exaggeration at sea-floor is about 2x.

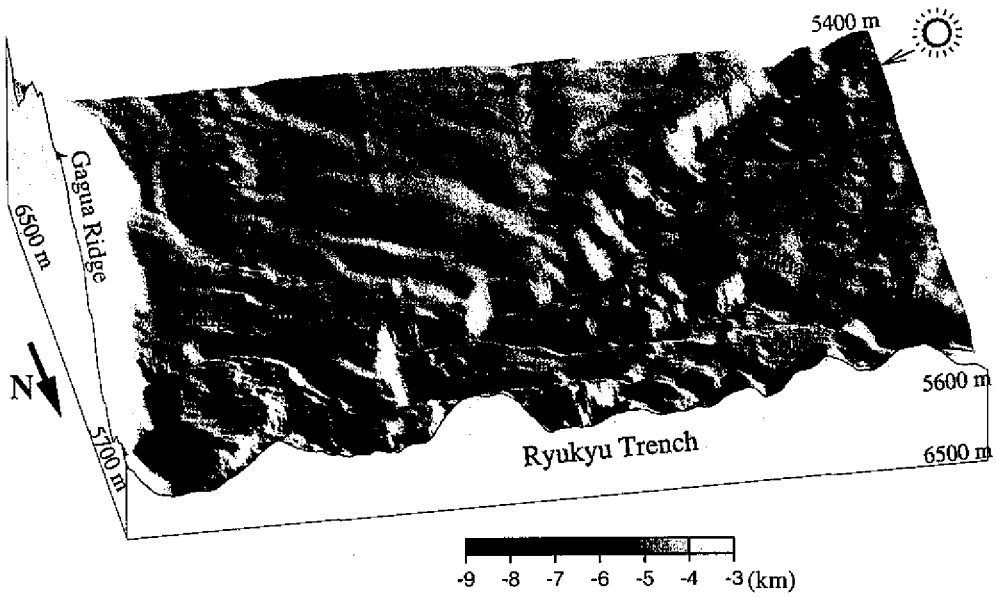

Fig. 10. Perspective shaded view of lower portion of the Taitung Canyon (section 4; see Figure 2 for location). The view is from the north (N10°), with a 30° elevation and N250° illumination angle. Water depths at the corners are indicated. The location of seismic profile 5 (line EW9509-05) is indicated by a dashed line.

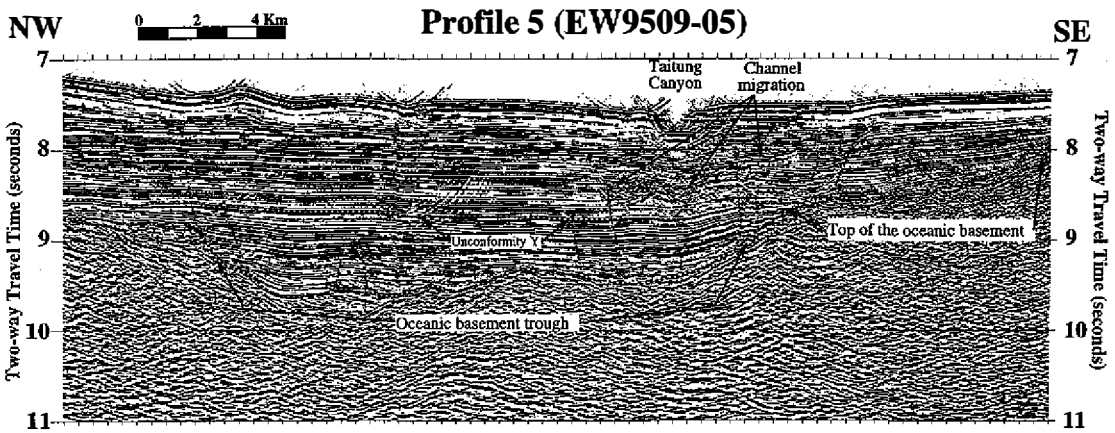

Fig. 11. Time-migrated seismic section of profile 4 (line EW9509-05). This profile runs SE-NW (see Figure 2 for location) across lower portion of the Taitung Canyon. Vertical exaggeration at sea-floor is about 2x.

Several authors have pointed out that the Philippine Sea plate is very likely to fail internally as a result of stresses generated in the collision zone along the Luzon arc as well as in the Ryukyu Trench. For example, earlier studies of the seismicity in the Huatung Basin (Wu, 1978; Wang, 1982) have proposed several NNW-SSE sinistral strike-slip faults, parallel to the N310° oriented relative convergence, while based on the alignment of the focal mechanisms, the possible existence of a WSW-ENE dextral strike-slip fault has also been mentioned (Hsu *et al.*, 1996; Sibuet and Hsu, 1996). Figure 12 shows the available focal mechanisms (Cheng, 1995; and CMT Worldwide Earthquakes Catalog) as well as the hypocenters (Cheng, 1995; and CNSS Worldwide Earthquake Catalog).

Furthermore, it has been proposed that the Luzon arc, between 22°25'N and 23°40'N, is dissected into two blocks about 60 to 80 km long (Malavieille *et al.*, 1997, Lallemand and Liu, 1998). The southern massif, just south of Lutao Island, may have undergone 5 to 10° of clockwise rotation but with little decrease in the convergence rate relative to the south China block compared to Lanyu. In the northern massif, the Coastal Range north of Taitung, NW-SE sinistral strike slip faults and NNE-SSW south-verging thrusts are documented (Lallemand and Liu, 1998), and since Late Pliocene, 25-30° clockwise rotation have occurred (Lee *et al.*, 1991). The segmentation pattern of the Luzon arc, within 22°25'N to 23°40'N, may well extend within the Huatung Basin. In particular, the rotation of southern massif could result into strike-slip faulting in the Huatung Basin initiating near the head of the Taitung Canyon.

In section 1 (Figure 12), seismic events may suggest strike-slip faults distributed in the head section of the Taitung Canyon. On seismic profile 1 (Figure 4), offset of the oceanic basement is visible at the southern and northern extremities of the seismic profile. The amount of offset in each region can't be quantified since accurate velocity information is lacking. Also, the sediment reflections lying on top of the basement appear rather continuous. In section 2, the seismicity appears to be concentrated on either the north and south sides away from the canyon but no fault outcrops can be identified from the bathymetric data. On seismic profiles 2 and 3 (Figures 6 and 8 respectively), normal faults of small thrown can be imaged underneath the canyon. Further east and in section 3, between 122°15'E and 122°32'E, almost no events are present in the vicinity of the Taitung Canyon (Figure 12). It is therefore difficult to assess the existence of strike-slip faulting in this area.

The Taitung Canyon flows rather continuously down slope in an ENE-ward direction until 122°35'E. On seismic profiles 2 and 3, the basement depth increases from north to south across the Taitung Canyon indicating a relative basement high on the southern side of the canyon. This high could be responsible for the northward shift of the canyon's path from 22°30'N to 22°35'N, characterized by a leftward bend in the center of section 2 and a rightward bend at the beginning of section 3.

The canyon's path is forced to turn NNE-ward as the canyon meets the basement high adjacent to the Gagua ridge (Figure 7). Although no outcrop of the basement is observed north of 22°50'N (Figure 9), the almost straight NNW path of the channel floor on Figure 2 seems to indicate that the canyon is still controlled by the basement high up to seismic profile 5. Furthermore, the 20 km wide trough in the oceanic basement imaged on seismic profile 4, where it is about 1.5 s TWT deep (Figure 9), extends northward as shown on seismic profile 5. At this

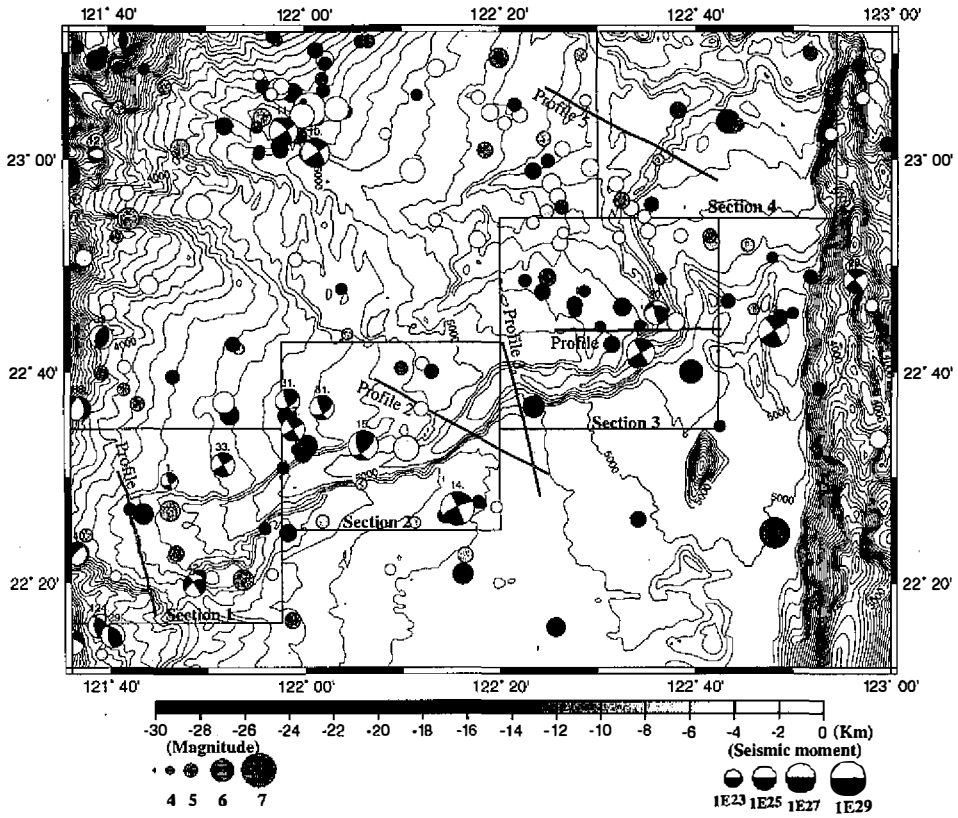

Fig. 12. Map of the shallow seismicity in the Huatung Basin. Focal mechanisms are taken from Cheng (1995), compiling ISC data (International Seismological Center) and CWBSN data (Central Weather Bureau Seismic Network) and from the CMT Worldwide Earthquakes Catalog. Events are scaled according to the seismic moment and depths are annotated on top of the beach ball. Hypocenters are taken from Cheng (1995) compiling TTSN data (Taiwan Telemetered Seismographic Network) and also provided by the Northern California Earthquake Data Center (CNSS Worldwide Earthquake Catalog). Events are scaled according to the square of their magnitude. Depths are indicated by gray scale between 0 and 30 km. Isobaths are in 100 m contours. The location of seismic profiles are indicated.

location, the trough is about 1 s TWT deep (Figure 11).

Moreover, seismicity is rather high in this area (Figure 12). Two clusters of shallow seismicity can be identified, running across the canyon in the center and at the end of section 3. However, the hypocenters are NNW trending rather then ENE. The alignments in a NNW

direction are consistent with SSE-NNW sinistral strike-slip faults at these locations. The outcrops of the elevated basement also have a NNW trend (Figure 7).

5. CONCLUSIONS

The structural features of the Taitung submarine canyon vary considerably along the 170 km course in the Huatung Basin from its head, between the volcanic islands of Lanyu and Lutao, to the Ryukyu Trench near the Gagua Ridge.

The Taitung Canyon crosses the Luzon volcanic arc and directs large volumes of sediment into the Huatung Basin. In the upper and central portion of the Taitung Canyon, although the canyon incises along steep levees the sediments in the surrounding Huatung Basin, the canyon is depositional by nature. Turbidite overspilling from the canyon appears to be the dominant mechanism for the fine deposit in the Huatung Basin. An asymmetric shape of the canyon walls is generally observed, in particular at bends in the channel's path.

Two unconformities have been identified in the Huatung Basin (Liu *et al.*, 1997). In the area of survey, the basin-wide unconformity Y is well expressed within the stratigraphy. Generally, the unconformity X coincides roughly with the floor of the Taitung Canyon and is particularly well imaged north-westerly to the path of the Taitung Canyon in the Huatung Basin.

On most seismic profiles, the Taitung Canyon is located above a depression in the top of the oceanic basement. Thus, a basement high, located to the south of the Taitung Canyon, could be responsible for the northward shift of the canyon's path near the end of section 2. In the third section, evidence for structural control by the basement is widespread, including a series oceanic basement ridges, which force the canyon's path to turn 90° towards the NNW. However, it is unclear whether these depressions originated during the formation of the oceanic crust or during more recent faulting. The thick overlying sediment sequences exhibit only minor, small displacement faults.

Active strike-slip faults in the oceanic basement may play an important role in the development of the Taitung Canyon. Thus, the local seismicity data may suggest dextral strike-slip faults oriented WSW-ENE in the vicinity of the canyon in sections 1 and 2. However, neither are such faults well expressed in the seismic profiles, nor are their outcrops visible in the bathymetric data. In section 3 and 4, analysis of the seismic profiles and the local seismicity data rather suggest a sinistral strike-slip fault system oriented SSE-NNW. Further investigation of the Huatung Basin should provide discriminate between the two compatible fault's orientations and their extensions in the basin, away from the Taitung Canyon.

Acknowledgments We would like to thank the crews and technical personnel of the R/V Maurice Ewing cruise EW9509, R/V l'Atalante cruise ACT, R/V Ocean Researcher I cruise ORI367, for their efforts in acquiring the data used in this study. Discussions with Y. Font, S.-K. Hsu, and H.-S. Yu, at the Institute of Oceanography, National Taiwan University, with G. F. Moore and N. Lundberg during the EW9509 cruise and with J. Malavieille, J. Angelier, J.-C. Sibuet, A. Deschamps during and after the ACT cruise have improved our understanding of the regional tectonic structures. G. F. Moore provided great help to our early steps with the ProMAX seismic data processing system. We are also grateful to G. F. Moore and L. S. Teng

for their constructive reviews. Maps where generated using GMT (Wessel and Smith, 1995). This study presents part of the results of the TAICRUST project jointly funded by the National Science Council, R.O.C. (grants NSC83-0209-M-002A-031Y, NSC83-0501-I-002-057-B42 and NSC84-0209-M-002A-001Y to C.-S. Liu) and the National Science Foundation, U.S.A. (grant OCE94-16583 to D. Reed, N. Lundberg and G. F. Moore).

REFERENCES

Angelier, J., 1986: Geodynamics of the Eurasia-Philippine Sea plate boundary . Preface. *Tectonophysics*, **125**, 1-33, IX-X.

Baraza, J., G. Ercilla, and the CAMEL shipboard party, 1997: The equatorial Atlantic mid-oceanic channel: an ultra high-resolution image of its burial history based on TOPAS profiles. *Mar. Geophys. Res.*, **19**, 115-135.

Biq, C. C., 1972: Dual-trench structure in the Taiwan-Luzon region. *Proc. Geol. Soc. China*, **15**, 65-75.

Bowin, C., Lu, R. S., Lee, C. S., and Schouten, H., 1978: Plate convergence and accretion in Taiwan-Luzon region. *Amer. Assoc. Petrol. Geol.*, **62**, no.9, 1654-1672.

Carlson, P. R., and H. A. Karl, 1988: Development of large submarine canyons in the Bering Sea, indicated by morphologic, seismic, and sedimentologic characteristics. *Geol. Soc. Am. Bull.*, **100**, 1594-1615.

Cheng, S. N., 1995: The study of stress distribution in and around Taiwan. Ph. D. Phesis, National Central University, Chung Li, Taiwan.

Damuth, J. E., R. D. Flood, R. O. Kowsmann, R. H. Belderson, and M.A. Gordini, 1988: Anatomy and growth pattern of the Amazon deep-sea fan as revealed by long-range side-scan sonar (GLORIA) and high resolution seismic studies. *AAPG Bull*, **72**, 885-911.

Deschamps, A., S. E. Lallemand, and J. Y., Collot, 1997: The tectonic significance of the Gagua Ridge near Taiwan. Abstract in *Tectonics of East Asia* (TEA) International Conference, Chung-Li, Taiwan, 3-5 Nov., 14222-143.

Dominguez, S., S. E. Lallemand, J. Malavieille, and P. Schnürle, 1998: Oblique subduction of the Gagua Ridge beneath the Ryukyu accretionary wedge system: Insight from marine observations and sandbox experiments, submitted to *Tectonics* .

Greene, G. H., S. H. Clarke, and M. P. Kennedy, 1991: Tectonic evolution of submarine canyons along the California continental margin. From Shoreline to abyss. *SEPM special publication*, **46**, 231-248.

Hagen, R. A., H. Vergara, and D. F. Naar, 1996: Morphology of San Antonio submarine canyon on the central Chile forearc. *Marine Geology*, **129**, 197-205.

Hagen, R. A., D. D. Bergersen, R. Moberly, and W. T. Coulbourn, 1994: Morphology of a large submarine canyon system on the Peru-Chile forearc. *Marine Geology*, **119**, 7-38.

Hilde, T. W. C., and C..S. Lee, 1984: Origin and evolution of the West Philippine Basin: A new interpretation;.*Tectonophysics*, **102**, 85-104.

Ho, C. S., 1986: A synthesis of the geological evolution of Taiwan. *Tectonophysics*, **125**, 1-

16.

Hsu, S. K., J. C. Sibuet, S. Monti, C. T. Shyu, and C. S. Liu, 1996: Transition between the Okinawa trough backarc extension and the Taiwan collision: new insights on the southernmost Ryukyu subduction zone. *Mar. Geophys. Res.*, **18**, 163-187.

Huang, C. Y., C. T. Shyu, S. B. Lin, T. Q. Lee, and D. D. Sheu, 1992: Marine geology in the arc-continent collision zone off southeastern Taiwan: Implications for Late Neogene evolution of the Coastal Range. *Mar. Geol.*, **107**, 183-212.

Karig, D. E., 1973: Plate convergence between the Philippines and the Ryukyu islands. *Mar. Geol.*, **14**, 153-168.

Karp, B. Y., R. Kulinich, C. T. Shyu, and C. S. Wang, 1997: Some features of the arc-continent collision in the Ryukyu subduction system, Taiwan junction area. In *The Island Arc*, **6**, 303-315.

Klaus, A., and B. Taylor, 1991: Submarine development in the Izu-Bonin forearc: a Sea MARC II and seismic survey of the Aoga Shima Canyon. *Mar. Geophys. Res.*, **13**, 131-152.

Lallemand, S. E., C. S. Liu, and ACT scientific crew, 1997: Swath bathymetry mapping reveals details of the active arc-continent collision offshore Taiwan. *EOS Tran., Am. Geophys. Un.*, **78 (17)**, 173-175.

Lallemand, S. E., and C. S. Liu, 1998: Geodynamic implications of present-day kinematics in the southern Ryukyus. *J. Geol. Soc. China* (accepted).

Lee, T. Q., C. Kissel, E. Barrier, C. Lai, and W. R. Chi, 1991: Paleomagnetic evidence for a diachronic clockwise rotation of the Coastal range. *Earth Planet. Sci. Lett.*, **104**, 245-257.

Liu, C. S., S. Y. Liu, S. E. Lallemand, D. Reed, and N. Lundberg, 1998: Digital elevation model offshore Taiwan and its tectonic implications. *TAO,* **9** (accepted).

Liu, C. S., S. E. Lallemand, S. J. Lin, P. Schnurle, and D. Reed, 1997: Forearc structures of the Ryukyu Subduction-Taiwan collision zone from seismic reflection studies east of Taiwan. AGU Fall meeting 1997.

Liu, C. S., P. Schnurle, S. E. Lallemand, and D. Reed, 1997a: Crustal structures of the Philippine Sea plate near Taiwan. Abstract in *Tectonics of East Asia* (TEA) International Conference, Chung-Li, Taiwan, 3-5 Nov. 1997, 54-55.

Liu, C. S., D. Reed, N. Lundberg, G. F. Moore, K. D. McIntosh, Y. Nakamura, T. K. Wang, T. H. Chen, and S. E. Lallemand, 1995: Deep seismic imaging of the Taiwan arc-continent collision zone. *EOS Tran., Am. Geophys. Un.*, **76 (46)**, F635.

Liu, C. S., N. Lundberg, D. Reed, and Y. L. Huang, 1993: Morphological and seismic characteristics of the Kaoping Submarine Canyon. *Mar. Geol.*, **111**, 93-108.

Lundberg, N., 1988: Present-day sediment transport paths south of the longitudinal valley, southeastern Taiwan. *Acta Geologica Taiwanica*, **26**, 317-331.

Lundberg, N., D. Reed, C. S. Liu, and J. Liekes, 1992: Structural controls on orogenic sedimentation, submarine Taiwan collision. *Acta Geologica Taiwanica*, **30**, 131-140.

Lundberg, N., D. Reed, C. S. Liu, and J. Liekes, 1997: Forearc-basin closure and arc accretion in the submarine suture zone south Taiwan. Special issue of *Tectonophysics* on Active Collision in Taiwan, **274**, 1/3, 5-24.

Ma, T. Y. H., 1947: Submarine valleys around the southern part of Taiwan and their geological significance. *Bull. Oceanographic Inst. Taiwan*, **2**, 1-12.

Ma, T. Y. H., 1963: Twin origin of the submarine canyons around Taiwan and the Quaternary glaciation in Taiwan as basis for refutation of the turbidity current theory and the so-called "great ice age" as due to universal lowering of temperature. *Petro. Geol. Taiwan*, **2**, 209-219.

Malavieille, J., S. E. Lallemand, and ACT scientific crew, 1997: Arc-Continent collision southeast of Taiwan: Preliminary results of the ACT cruise. Abstract in *Terra Nova*, **9**, suppl. on EUG 9 Conference, Strasbourg 23-27 March, 339.

Menard, H. W., 1955: Deep-sea channels, topography and sedimentation. *Bull. Amer. Assoc. Petrol. Geol.*, **39**, (2), 236-255.

Mrozowski C. L., S. D. Lewis, and D. E. Hayes, 1982: Complexities in the tectonic evolution of the West Philippine Basin. *Tectonophysics*, **82**, 1-24.

Nagel, D. K., H. T. Mullins, and H. G. Greene, 1986: Ascension Submarine Canyon, California - Evolution of a multi-head canyon system along a strike-slip continental margin. *Mar. Geol.*, **73**, 285-310.

Pratson, L. F., and M. H. Edwards, 1996: Introduction to advance seafloor mapping using sidescan sonar and multibeam bathymetry data. *Mar. Geophys. Res.*, **18**, 601-605.

Pratson, L. F., and W. B. F. Ryan, 1996: Automated drainage extraction in mapping the Monterey submarine drainage system, California margin. *Mar. Geophys. Res.*, **18**, 757-777.

Reed, D., N. Lundberg, C. S. Liu, and B. Y. Kuo, 1992: Structural relations along the margins of the offshore Taiwan accretionary wedge: Implications for accretion and crustal kinematics. *Acta Geologica Taiwanica*, **30**, 105-122.

Schnürle, P., C. S. Liu, S. E. Lallemand, and D. Reed, 1998: Structural insight into the south Ryukyu margin: Effects of the subducting Gagua Ridge. In "Deep seismic profiling of the continents, II: A global survey". *Tectonophysics*, **288**, 237-250.

Seno, T., S. Stein, and A. E. Gripp, 1993: A model for the motion of the Philippine Sea Plate with NUVEL-1 and Geological data. *J. Geophys. Res.*, **98**, 17941-17948.

Shepard, F. P., and R. F. Dill, 1966: Submarine canyons and other sea valleys, *R. McNally & Co.*, Chicago, pp. 381.

Sibuet, J. C., and S. K. Hsu, 1996: Geodynamics of the Taiwan arc-arc collision. *Tectonophysics*, **274**, 221-251.

Soh, W., H. Tokuyama, K. Fujioka, S. Kato, and A. Taira, 1990: Morphology and development of a deep-sea meandering canyon (Boso Canyon) on an active plate margin, Sagami Trough, Japan. *Marine Geology*, **91**, 227-241.

Soubaras, R., 1992: Explicit 3D migration using equiripple polynomial expansion and Laplacian synthesis. SEG Annual Meeting Expanded Abstracts, 905-908.

Suppe, J., 1987: The active Taiwan mountain belt. In: J. P. Schaer and J. Rodgers (Eds.), Comparative Anatomy of Mountain Ranges, Princeton University Press, 277-293.

Teng, L. S., 1995: Neotectonics of northern Taiwan and southern Ryukyu. In: Sino-French Symposium on Active Colision in Taiwan, Taiwan, 287-292.

Teng, L. S., 1990: Geotectonic evolution of late Cenozoic arc-continent collision in Taiwan. *Tectonophysics*, **183**, 57-76.

Yu, H. S., and C.,S., Chiang, 1997: Kaoping Shelf: morphology and tectonic significance. *J. Southeast Asian Earth Sci.*, **13**, 9-18.

Yu, S. B., H. Y. Chen, and L. C. Kuo, 1997: Velocity field of GPS stations in the Taiwan area. Special issue of *Tectonophysics* on Active Collision in Taiwan, **274**,1/3, 41-59.

Yu, S. B., and H. Y. Chen, 1994: Global Positioning System measurements of crustal deformation in the Taiwan arc-continent collision zone. *TAO*, **5**, 477-498.

Wang, C. S., 1982: Earthquakes caused by horizontal bending of the Philippine Sea plate near Taiwan. *Tectonophysics*, **88**, T1-T6.

Wessel, P. and W. H. F. Smith, 1991: The GMT-System Version 2.0, Technical Reference and Cookbook. Scripps Institution of Oceanography, Univ. California, San Diego.

Wu, F. T., 1978: Recent tectonics of Taiwan. *J. Physics Earth*, **26** (Suppl.), S265-99.